LETTERS TO THE EDITOR

The Letters to the Editor section is divided into four categories entitled Communications, Notes, Comments, and Errata. Communications are limited to three and one half journal pages, and Notes, Comments, and Errata are limited to one and three-fourths journal pages as described in the Announcement in the 1 July 1996 issue.

COMMUNICATIONS

Nonadiabatic wave packet dynamics: Predissociation of IBr

Marc J. J. Vrakking,[a] D. M. Villeneuve, and Albert Stolow
Steacie Institute for Molecular Sciences, National Research Council of Canada, Ottawa, Ontario, Canada K1A OR6

We present results of fs pump–probe experiments on the predissociation dynamics of the IBr B-state, as a model of nonadiabatic wave packet dynamics on coupled potential energy curves. The observations reflect the complicated wave packet motion on the coupled potentials and oscillatory behavior of the decay rates as a function of excitation energy. © *1996 American Institute of Physics.* [S0021-9606(96)02836-X]

With the advent of ultrafast laser techniques, which allow the probing of molecular motion on femtosecond time scales, new kinds of studies of complicated non-Born–Oppenheimer (B–O) photochemical events like intersystem crossing and internal conversion have become possible. An exciting result of a number of these studies is that even in complex molecular systems, the dynamics can frequently be described in terms of low-dimensional wave packet motion on a limited number of potential energy surfaces.[1–3]

Wave packet motion in diatomic molecules represents the simplest model system where curve-crossing manifests itself and, as such, serves as a basis for understanding the low-dimensionality approximation often used in polyatomic nonadiabatic effects. Wave packet experiments in diatomic molecules have been carried out on systems such as I_2 or Na_2 that can be described by a single potential energy curve[4,5] or systems like NaI, where two diabatic potential energy curves are strongly coupled.[6,7] In this communication, we present experimental fs pump–probe studies on the IBr molecule, where a complicated wave packet evolution is observed which cannot be described exclusively by either the diabatic (weak coupling) or adiabatic (strong coupling) pictures.[8–10]

In Fig. 1 both diabatic (dashed lines) and adiabatic (solid lines) potential energy curves are shown for the IBr molecule. The diabatic bound $B(^3\Pi_0^+)$ and repulsive $B'(O^+)$ state potential energy curves are obtained in the B–O approximation. This approximation breaks down near the crossing point, where coupling between the two states leads to considerable mixing of the two diabatic configurations. As a result, adiabatic potential energy curves may be defined and these are shown as the solid lines in Fig. 1. The lower adiabatic curve is unbound at energies above the crossing point, whereas the upper adiabatic curve is a bound state which is capable of supporting vibrational levels.

The $B(^3\Pi_0^+) \leftarrow X(^1\Sigma^+)$ absorption spectrum of the IBr

molecule presented spectroscopists with an interesting challenge. The spectrum contains a large number of diffuse bands and there exist only a limited number of regions where sharp rotational structure can be observed.[11] An interpretation of the spectrum was given by Child:[12–14] the large majority of rovibrational states rapidly predissociate via coupling to the repulsive $B'(O^+)$ state, which intersects the $B(^3\Pi_0^+)$ state above $v'=5$. Sharp lines in the absorption spectrum arise from a near-resonance between ro-vibrational levels in the bound diabatic $B(^3\Pi_0^+)$ state potential well
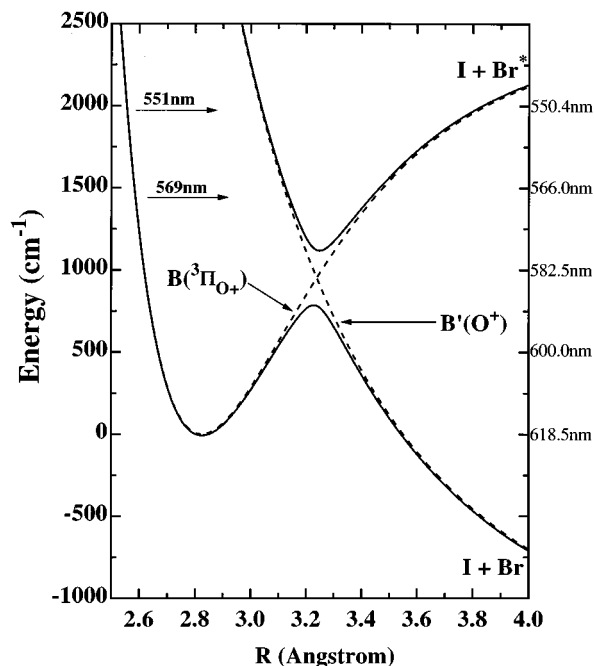
FIG. 1. Relevant potential energy curves for the intermediate case IBr molecule. The diabatic potential energy curves (dotted lines) were taken from Ref. 10. The adiabatic potential energy curve (solid lines) were calculated using an R-independent coupling strength of 170 cm^{-1}. The pump wavelength scale is shown on the right. The two particular pump wavelengths, 551 and 569 nm, used in this experiment are indicated by arrows.

[a]Present address: Department of Chemistry, Free University Amsterdam de Boelelaan 1083, 1081HV Amsterdam, The Netherlands.

(Fig. 1; dotted line) and the upper adiabatic potential well (Fig. 1; upper solid line). The onset for rapid predissociation is at the crossing point between the two diabatic curves (adiabaticlike behavior), whereas photodissociation at excitation energies above the dissociation threshold for formation of I+Br* leads predominantly to the production of I+Br* rather than I+Br (diabaticlike behavior).[15,16] This suggests that the dissociation dynamics involves a mixture of the diabatic and adiabatic pictures, i.e., the intermediate case. In support of this, the (few) observed rotational levels lead to constants which are found to be intermediate between those expected based on the energy minima of either the diabatic or adiabatic potential wells. The resonance Raman spectrum of IBr[9] was recorded and theoretically modelled both above and below the B-state dissociation threshold, showing clearly effects due to curve crossing.

We performed fs pump–probe experiments on IBr in order to single out the purely vibrational dynamics which manifests itself at short times. In these experiments, rotationally cold IBr molecules were excited from the ground state (r_e=2.47 A) to the inner turning point of the diabatic $B(^3\Pi_0^+)$ state potential well using a tunable fs laser pulse. The ensuing wave packet evolution was monitored by measuring the return of the wave packet to the inner turning point of the $B(^3\Pi_0^+)$ state potential well using two-photon ionization with a second fs laser pulse. Experiments were carried out over a wide range (547–590 nm) of excitation energies: from the crossing point of the two diabats to near the I+Br* dissociation threshold. The observed wave packet motion was found to vary strongly with the excitation energy. Oscillatory behavior of the predissociation rate as a function of vibrational excitation was inferred, as was noted by Guo.[10]

We briefly describe the experimental apparatus.[17,18] A Ti–sapphire fs oscillator was amplified using a synchronized ps Nd:YAG laser.[19] The amplified fs pulse was split and used to generate two white light continua from which the required colors for the pump and probe lasers were selected and reamplified. The central pump wavelength was varied from 547 nm to 590 nm. For the probe laser, light around a central wavelength of 680 nm was selected, and frequency doubled in a 0.1 mm BBO crystal, giving a 100 fs pulse centered around 340 nm. The pump and probe lasers were attenuated to approximately 25 and 10 μJ/pulse, respectively, and combined using a dichroic beamsplitter. The collinear, co-propagating fs lasers were then focused into the molecular beam apparatus. Care was taken to locate the foci of the visible and uv laser beams away from the molecular beam axis so that neither the visible nor the two-photon ultraviolet transitions were saturated.

IBr$^+$ ions were collected as a function of the time delay between the pump and probe lasers, which was varied between 0 and 30 ps using a motorized delay stage in the pump laser path. The partial pressure of the IBr sample (Aldrich), which was used without further purification, was controlled to 20 Torr and the IBr was rotationally cooled by seeding in 1 atmosphere of He. Care was taken to shield the IBr sample
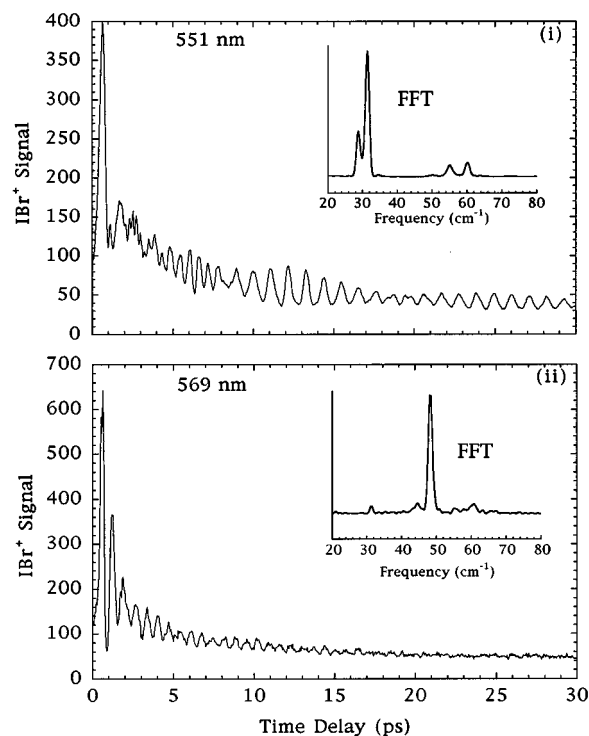
FIG. 2. (i) Time delay scan showing the measured IBr$^+$ signal as a function of the time delay between the one-photon pump excitation and the two-photon probe step, for a pump wavelength of 551 nm and a probe wavelength of 340 nm. In the inset, the FT is presented showing nearest-neighbor coherences near 30 cm^{-1} and next-nearest-neighbor coherences near 60 cm^{-1}, involving states near v'=27. (ii) Time delay scan showing the measured IBr$^+$ signal as a function of time delay for a pump wavelength of 569 nm and a probe wavelength of 340 nm. The inset shows the FT which contains a single nearest-neighbor coherence near 48 cm^{-1}, involving states near v'=20.

and the gas lines connecting the sample to the molecular beam apparatus from ambient roomlight.

In Fig. 2(i), the detected IBr$^+$ signal is shown as a function of the delay between the pump and probe lasers for a central pump wavelength of 551 nm. The signal contains a large number of reproducible oscillations, which appear irregular at shorter and regular at longer time delays. The pump–probe signal shows an overall decay, which reflects the predissociation of the excited state. It is interesting that the long time behavior shown in Fig. 2(i) indicates that a portion of the excited state population persists on a significantly longer time scale. (A simple Landau–Zener calculation suggests that once per vibrational period, 39% of the population dissociates and, therefore, that the excited molecule is expected to decay within a few vibrational periods.)

The fs pump laser excites a wave packet which consists of a coherent superposition of vibrational states. If these states endure on the time scale of the experiment, then one expects a Fourier transform power spectrum (FT) to show the presence of sharp frequency components corresponding to energy differences between any two pairs of states in the coherent superposition. In the current experiment, the bandwidth of the pump laser (about 200 cm^{-1}) was sufficient to coherently excite 6 to 8 vibrational levels. However, as the

FT of the time delay scan (inset) shows, the number of sharp peaks observed is significantly less. Only two peaks are observed near 30 cm^{-1}, corresponding to coherences between neighboring vibrational levels which are tentatively assigned as coherences between $v'=27$ and $v'=28$ ($\Delta E=28.65$ cm^{-1}) and between $v'=26$ and $v'=27$ ($\Delta E=31.25$ cm^{-1}), using the data of Eberhardt and Sullivan.[20] In addition, two peaks are seen which are tentatively assigned as coherences between $v'=27$ and $v'=29$ ($\Delta E=55.15$ cm^{-1}) and $v'=26$ and $v'=28$ ($\Delta E=60.55$ cm^{-1}). We conclude that only a limited number of vibrational states in the vicinity of $v'=27$ have sufficiently long predissociation lifetimes to manifest themselves in the FT. At short times (0–5 ps) the wave packet consists of a larger number of vibrational states and the structure of the wave packet as reflected in the pump–probe signal rapidly becomes very complicated because twice per vibrational period (1 ps at this excitation energy) the wave packet moves through the crossing region and splits into two smaller wave packets. At longer times, a significant number of vibrational states in the coherent superposition have decayed and only a few levels have any significant residual population, resulting in a simplified beat structure.

In Fig. 2(ii), the detected IBr$^+$ signal is shown as a function of the delay between the pump and probe lasers for excitation centered around 569 nm. The overall decay of the pump–probe signal is significantly faster than at 551 nm and, furthermore, the time delay scan and the FT (inset) now show the presence of just a single component at a frequency of approximately 48.15 cm^{-1}, corresponding to a nearest-neighbor coherence in the vicinity of $v'=20$. As in our earlier discussion of the measurements at 551 nm, we conclude that the prepared coherent superposition of vibrational states (approximately 5 to 6 levels at this pump wavelength) contains only a single pair of neighboring vibrational states with long enough lifetimes for the coherence between them to be observed.

The nearest-neighbor coherences of the experiments at 551 nm and at 569 nm are in fact the *only* nearest-neighbor coherences that were observed in these experiments (in the pump laser wavelength range 547 nm to 590 nm). Nearest-neighbor coherences at 28.65, 31.25, 33.9 cm^{-1} were observable in scans with pump wavelengths between 551 nm and 564 nm, and the nearest-neighbor coherence at 48.15 cm^{-1} was observable in scans at pump wavelengths between 559 nm and 572 nm. Thus, the experiments suggest that the predissociation lifetimes oscillate as a function of vibrational excitation, becoming relatively longer in the vicinities of $v'=20$ and $v'=27$. In a wave packet description, the wave packet evolving on the diabatic $B(^3\Pi_0^+)$ state interferes with the wave packet evolving on the upper adiabat. This interference can lead, for characteristic energies, to standing waves which represent the long-lived resonances.

The simplified beat structure which is observed in Fig. 2(i) following the partial initial decay of the wave packet is reminiscent of the structure seen in the experiments of Zewail and co-workers on the predissociation dynamics of NaI.[21] Their origin, however, is different. In NaI, revival-like structures appear after about 20 ps, although from the poten-
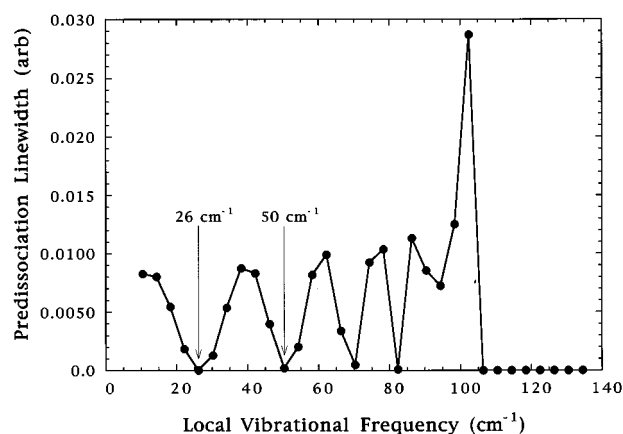
FIG. 3. Calculated predissociation linewidths of the vibrational levels belonging to the diabatic $B(^3\Pi_0^+)$ potential energy curve, calculated using Fermi's golden rule by application of the uniform Airy approximation. The level widths are plotted versus the local vibrational frequency (i.e., local level spacing). The arrows indicate the minima in the predissociation linewidths, corresponding to the long-lived resonances observed in the experiment.

tial a revival time of 300 ps would be expected. This structure is due to a beat between two slightly different classical periods belonging to subsets of the original wave packet that are left over once the central frequency components of the wave packet has decayed.[8,22,23] By contrast, in IBr, after the initial ultrafast decay a wave packet with a *single* classical period is left over. The revival-like structures of the IBr wave packet therefore follow the conventional definitions of revivals,[24,25] the revival period being estimated to be about 26 ps. (At a revival, the phase relationship between vibrational states is the same as it was at $\Delta t=0$.)

In the remainder of this paper, a simple interpretation of the existence of sharp resonances at specific levels of vibrational excitation is presented using a treatment, however, which applies to weakly coupled diabatic potential energy surfaces. The validity of this approach, based on Fermi's golden rule, is limited because of the strength of the interaction between the $B(^3\Pi_0^+)$ state and the $B'(O^+)$ state (170 cm^{-1}). Nevertheless, using this approach, sharp resonances are predicted in qualitative agreement with the experimental results.

In the limit of weak coupling between a bound state and a dissociative continuum, the predissociation level width is given by Fermi's golden rule. The decay rate depends on the overlap of the vibrational and continuum wavefunction, mediated by the coupling. The level widths were evaluated using the uniform Airy approximation,[8,26–28] yielding the result that the predissociation rate is a very rapidly oscillating function of excitation energy. The widths of the predissociating levels of the $B(^3\Pi_0^+)$ state were determining by combining the results of the uniform Airy approximation with the discrete level structure of the $B(^3\Pi_0^+)$ state potential well, which was calculated by solving the time-independent Schrödinger equation numerically.[29] The results of these calculations, which were obtained using diabatic potential energy curves of Guo,[10] are shown in Fig. 3. The level widths

of the predissociating vibrational levels of the $B(^3\Pi_0^+)$ state are shown as a function of the local vibrational frequency, i.e., the level spacing between the vibrational level under consideration and its higher nearest neighbor. This method of displaying the level widths is appropriate here, since the FT of fs pump–probe experiments yields frequencies corresponding to level spacings between adjacent vibrational levels, i.e., at the local vibrational frequency. Figure 3 clearly illustrates how the level widths display oscillatory behavior as a function of the vibrational quantum number and, therefore, the local vibrational frequency. These oscillations have also been noted by Guo.[10] In our experiments, vibrational levels with finite predissociation lifetimes were observed near $v'=20$ and $v'=27$, where the local vibrational frequencies were approximately 48 cm^{-1} and 30 cm^{-1}, respectively. Due to the weak coupling approximation, we do not expect the overall form of the oscillations in Fig. 3 to be accurate. However, the observed frequencies correspond very nicely to two consecutive minima in Fig. 3, indicated by arrows, supporting the interpretation of the data that in our fs pump–probe experiments coherences are only seen for *pairs* of states whose predissociation level widths are small. We note that the calculation predicts that additional Fourier components might be seen near 70 and 82 cm^{-1}. Experimentally, these peaks were not observed, which may be related to the fact that the observation of a Fourier component requires a long predissociation lifetime for *two* neighboring vibrational levels rather than just one.

In conclusion, in this communication we have presented results of fs pump–probe experiments on nonadiabatic dynamics in a model system, the IBr molecule. The observed wave packet dynamics is complicated as a consequence of the intermediate strength coupling between the diabatic $B(^3\Pi_0^+)$ and $B'(O^+)$ states. In such a case, neither a diabatic nor an adiabatic description of the dynamics is appropriate. The experiments suggest that the decay rates of vibrational eigenstates on the coupled potential energy surfaces display oscillatory behavior as a function of excitation energy. These experiments provide details of nonadiabatic wave packet evolution in diatomic molecules and illustrate the utility of time-domain techniques for observing broad ranges of resonance lifetimes. Hopefully, these studies will foster more research into nonadiabatic wave packet phenomena in larger molecules.

[1] See, for example, R. Schinke, *Photodissociation Dynamics* (Cambridge University Press, Cambridge, England, 1993).

[2] A. Zewail, *Femtochemistry: Ultrafast Dynamics of the Chemical Bond* (World Scientific, Singapore, 1994).

[3] *Femtosecond Chemistry*, edited by J. Manz and L. Wöste (VCH, Weinheim, 1995).

[4] M. Gruebele and A. H. Zewail, J. Chem. Phys. **98**, 883 (1993).

[5] T. Baumert *et al.*, in Ref. 3, p. 397.

[6] T. S Rose, M. J. Rosker, and A. H. Zewail, J. Chem. Phys. **88**, 6672 (1988); **91**, 7415 (1989); Chem. Phys. Lett. **146**, 175 (1988).

[7] Ch. Meier, V. Engel, and J. S. Briggs, J. Chem. Phys. **95**, 7337 (1991).

[8] M. Baer and M. S. Child, Mol. Phys. **36**, 1449 (1978).

[9] I. Levy, M. Shapiro, and A. Yogev, J. Chem. Phys. **96**, 1858 (1992); H. Bony, M. Shapiro, and A. Yogev, Chem. Phys. Lett. **107**, 603 (1984).

[10] H. Guo, J. Chem. Phys. **99**, 1685 (1993).

[11] L.-E. Selin, Ark. Fysik **21**, 529 (1962).

[12] A. D. Bandrauk and M. S. Child, Mol. Phys. **19**, 95 (1970).

[13] M. S. Child and R. B. Bernstein, J. Chem. Phys. **59**, 5916 (1973).

[14] M. S. Child, Mol. Phys. **32**, 1495 (1976).

[15] M. S. de Vries, N. J. A. Veen, and A. E. de Vries, Chem. Phys. Lett. **56**, 15 (1978).

[16] M. S. de Vries *et al.*, Chem. Phys. **51**, 159 (1980).

[17] I. Fischer *et al.*, J. Chem. Phys. **102**, 5566 (1995).

[18] I. Fischer *et al.*, Chem. Phys. **207**, 331 (1996).

[19] D. M. Villeneuve, I. Fischer, and A. Stolow, Opt. Commun. **114**, 141 (1995).

[20] W. H. Eberhardt and W. Sullivan, J. Mol. Spectrosc. **70**, 270 (1978).

[21] P. Cong, A. Mokhtari, and A. H. Zewail, Chem. Phys. Lett. **172**, 109 (1990).

[22] J. R. Waldeck, M. Shapiro, and R. Bersohn, J. Chem. Phys. **99**, 5924 (1993); M. Shapiro, Faraday Discuss. Chem. Soc. **91**, 352 (1991).

[23] S. Chapman and M. S. Child, J. Phys. Chem. **95**, 578 (1991).

[24] I. Sh. Averbukh and N. F. Perel'man, Sov. Phys. Usp. **34**, 572 (1991).

[25] M. J. J. Vrakking, D. M. Villeneuve, and A. Stolow, Phys. Rev. A **54**, R37 (1996).

[26] W. H. Miller, J. Chem. Phys. **48**, 484 (1968).

[27] M. S. Child, J. Phys. B **13**, 2557 (1980).

[28] M. S. Child, in *Semiclassical Methods in Molecular Scattering and Spectroscopy* (Reidel, New York, 1980).

[29] J. W. Cooley, Math. Comput. **XV**, 363 (1961).